First-principles study of the electronic and magnetic properties of $Sr_2Fe_{1+x}Mo_{1-x}O_6$

2008 J. Phys.: Condens. Matter 20 075218

(http://iopscience.iop.org/0953-8984/20/7/075218)

J. Phys.: Condens. Matter **20** (2008) 075218 (6pp) doi:10.1088/0953-8984/20/7/075218

First-principles study of the electronic and magnetic properties of $Sr_2Fe_{1+x}Mo_{1-x}O_6$

X F Zhu[1], Q F Li[1,2] and L F Chen[1]

[1] Department of Physics, Nanjing Normal University, Nanjing 210097, People's Republic of China
[2] Department of Physics, Nanjing University of Information Science and Technology, Nanjing 210044, People's Republic of China

Received 18 September 2007, in final form 7 December 2007
Published 28 January 2008
Online at stacks.iop.org/JPhysCM/20/075218

Abstract

We have investigated the electronic and magnetic properties of $Sr_2Fe_{1+x}Mo_{1-x}O_6(-1 \leqslant x \leqslant 0.25)$, the composition $x = 0$ corresponding to the well-known double perovskite system Sr_2FeMoO_6, using first-principles density functional theory within the generalized gradient approximation (GGA) + U schemes. The crystal structure of the compounds has a cubic lattice for $x = -1$ and 0.25 while the structure of the compounds has a tetragonal lattice from $x = -0.75$ to 0.0. The lattice parameters decrease slightly as the Fe content increases and the variation of unit cell volume is linear with the composition x. Our spin-polarized calculations give a metallic ground state for the $x < 0$ regime and a half-metallic ground state for the $x \geqslant 0$ regime. The magnetic structures for $x \leqslant 0$ are found to be the ferromagnetic state while the magnetic structure for $x = 0.25$ is the ferrimagnetic state where any Fe at the Mo crystallographic site is coupled antiparallel to the Fe moments at the correct site.

(Some figures in this article are in colour only in the electronic version)

1. Introduction

Half-metallic ferromagnetic oxides [1] have attracted extensive attention not only as a source of fully polarized charge carriers for spintronics applications but also as potential candidates for memory devices by the virtue of their large magnetoresistance (MR). Recently, a double perovskite Sr_2FeMoO_6, belonging to this general family of half-metallic ferromagnetic oxides, has shown spectacularly large MR even at room temperature and at relatively small applied magnetic fields [2] compared to the extensively investigated class of magnetoresistive manganites, due to its substantially enhanced Curie temperature (T_c). The enhanced T_c and the origin of ferromagnetism in Sr_2FeMoO_6 and related compounds have been explained [3] in terms of a kinetically driven mechanism.

A perfectly ordered lattice of Sr_2FeMoO_6 consists of alternating FeO_6 and MoO_6 octahedra along all the three cubic axes of the perovskite structure (see figure 1). The structural and electronic properties of Sr_2FeMoO_6 have been extensively investigated by a number of research groups [2–4]. It is believed that the fully ordered compound is a half-metallic ferromagnet with nominal ionic configurations of Fe^{3+} and Mo^{5+}. The measured value of the saturation magnetization M_s in normally prepared samples is invariably found [2, 5, 6] to be lower than the expected value of 4 μ_B per formula unit (f.u.) from the half-metallic state. This is due to the inevitable presence of mis-site disorders, where some Fe and Mo interchange their crystallographic positions. However, the microscopic origin of the reduction in M_s is still not entirely clear. Both classical Monte Carlo simulations [7] and quantum-mechanical band-structure calculations [8] indeed predicted a reduction of M_s as a function of mis-site disorder, but the underlying reasons for this reduction are very different in these two proposals. In one case [7] it is assumed that the moment reduction is only due to antiferromagnetically coupled Fe pairs whenever Fe–O–Fe bonds are generated by such mis-site disorders. In this view, the conduction band presumably retains its polarization to a large extent. In contrast, the band-structure approach [8] attributed the reduction of the moment to strong depolarization effects at each site, though all Fe sites were found to be ferromagnetically coupled. The mis-site disorder and its effect on the conduction band are not only important in the context of spin-injection devices; the magnetoresistive properties of these samples also appear to

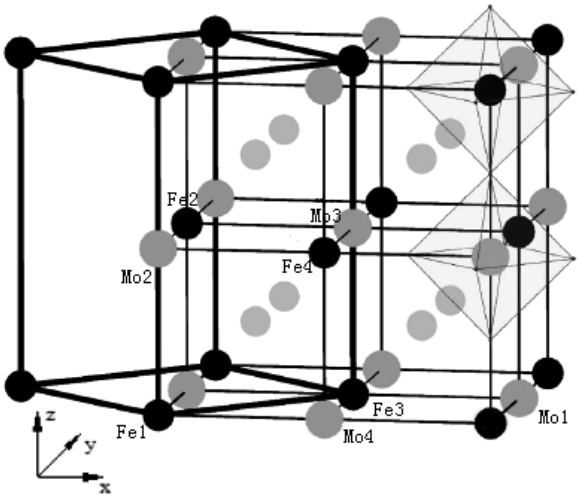

Figure 1. The ideal crystal structure of double perovskite Sr_2FeMoO_6; Fe (black), Mo (dark gray), Sr (light gray), and O (octahedra); the cubic lattice is drawn in thin black lines, the tetragonal lattice in thick black lines. This cubic structure can be well described within the $Fm3m$ space group. Note also the notions of atoms used in the analysis of electronic and magnetic structures in figure 4 and table 2.

be strongly influenced by these factors [9]. Therefore, it is important to investigate theoretically the underlying details of the magnetic structure and the effect of mis-site disorder to obtain a definitive understanding of magnetism in this class of compounds.

In this paper we study the electronic and magnetic structure of $Sr_2Fe_{1+x}Mo_{1-x}O_6(-1 \leqslant x \leqslant 0.25)$ by generalized gradient approximation (GGA)+U band-structure calculations. The on-site Coulomb energy U has been taken into account to unravel the correlation effects of the localized d orbital on magnetic moments as well as on the electronic structures. The remainder of the paper is organized as follows. Section 2 describes our computational details. The results and discussions are presented in section 3. Section 4 gives a brief summary of this work.

2. Computational details

First-principles calculations of $Sr_2Fe_{1+x}Mo_{1-x}O_6$ are performed in a plane-wave basis set using the projector augmented wave (PAW) [10, 11] method in the generalized gradient approximation (GGA) as it is implemented in the Vienna *ab initio* simulation program (VASP) [12, 13]. The local spin density approximation (LSDA) and GGA are known to fail in the description of the electronic properties of early transition metal (TM) compounds, as the electron self-interaction error, always present in these formulations, becomes significant for electrons in the well-localized TM d levels. Thus we have employed the DFT + U [14–17] methodology which is able to significantly improve predictions of phase stability and thermodynamic properties as well as magnetic and electronic structure in oxides. We use here the simple formulation by Liechtenstein *et al* [16] and Dudarev *et al* [17], where a single parameter U_{eff} determines an orbital-dependent correction to the density functional theory (DFT) energy. U_{eff} is generally expressed as the difference between two parameters, the Hubbard U, which is the Coulomb-energetic cost of placing two electrons at the same site, and an approximation of the Stoner exchange parameter J, which is almost constant at 1 eV.

To study the electronic and magnetic properties of $Sr_2Fe_{1+x}Mo_{1-x}O_6(-1 \leqslant x \leqslant 0.25)$, we have constructed a supercell consisting of 40 atoms. Calculations are performed by constructing supercells of four formula units with four inequivalent Fe sites at (0, 0, 0), (0, 0.5, 0.5), (0.5, 0.5, 0), and (0.5, 0, 0.5) positions and four inequivalent Mo sites at (0, 0.5, 0), (0, 0, 0.5), (0.5, 0.5, 0.5), and (0.5, 0, 0) positions for the ordered sample as shown in figure 1. These inequivalent Fe and Mo sites are designated as Fe1, Fe2, Fe3, and Fe4 and Mo1, Mo2, Mo3, and Mo4, respectively. The ideal $x = 0$ composition corresponds to the maximal Fe content possible in this crystal structure, while avoiding a nearest-neighbor Fe–O–Fe arrangement. Therefore, in the Fe-deficient regime ($x < 0$) we control the average separation between the magnetic ions by changing x. In the Fe-rich composition ($x > 0$), we replace some of the Mo with Fe in the ordered structure, thereby forcing the additional Fe ions necessarily to form Fe–O–Fe 180° bonds. Thus, we obtain a control on number of such bonds introduced in the system by controlling x. The internal coordinates and cell parameters are fully relaxed. The Brillouin zone integration is performed using Monkhorst–Pack grids [18] and the tetrahedron method with Blöchl corrections is used for calculation of the total energy. The number of plane waves in VASP is controlled by the cut-off energy, which in all our static calculations was 400 eV, while all the geometry relaxations were performed with an increased cut-off of 520 eV to ensure proper convergence of the stress tensor. Forces on atoms were calculated, and atoms were allowed to relax using a conjugate gradient technique until their residual forces had converged to less than 0.01 eV $Å^{-1}$. To explore the effects of the on-site Coulomb energy U on the electronic structures and the magnetic moments, specific values for Fe ($U = 3.0$ eV and $J = 0.9$ eV) are used and taken as an averaged effective U value of U_{eff} (Fe) = 2.10 eV.

3. Results and discussion

3.1. Structure relaxation

We show our calculated relaxed structural parameters for different compositions by using the GGA + U method in table 1. The unit cell shape, lattice vectors, and atomic coordinates were optimized simultaneously. The crystal structure of the compounds for $x = -1$ and 0.25 has a cubic lattice while the crystal structure of the compounds from $x = -0.75$ to 0.0 has a tetragonal lattice. Recent group theoretical analysis shows that $I4/m$ is the most probable space group for $x = 0$ materials [19]. The cell volume decreases over a wide range of compositions ($-1 \leqslant x \leqslant 0.25$). The mean bond distance $d_{\langle \text{Fe—O} \rangle}$ increases in the Fe-deficient composition ($x < 0$) while it decreases in the Fe-rich composition ($x > 0$). The mean bond distance $d_{\langle \text{Mo–O} \rangle}$ decreases from 2.008 Å for $x = -1$ to 1.950 Å for $x = 0.25$. The relaxed bond angles

Table 1. Calculated structural parameters and total magnetic moments for $Sr_2Fe_{1+x}Mo_{1-x}O_6$ ($-1 \leqslant x \leqslant 0.25$).

Composition, x	-1.0	-0.75	-0.5	-0.25	0.0	0.25
a (Å)	8.031	8.016	7.984	7.989	7.974	7.958
b (Å)	8.031	8.016	7.984	7.989	7.974	7.958
c (Å)	8.031	8.013	8.037	7.990	7.978	7.958
V (Å^3)	517.92	514.86	512.32	510.00	507.31	504.04
$d_{\langle Fe-O\rangle}$ (Å)	—	2.018	2.024	2.027	2.028	2.013
$d_{\langle Mo-O\rangle}$ (Å)	2.008	2.002	1.991	1.981	1.960	1.950
μ_T (μ_B/f.u.)	0.00	1.29	2.40	3.25	4.00	3.50

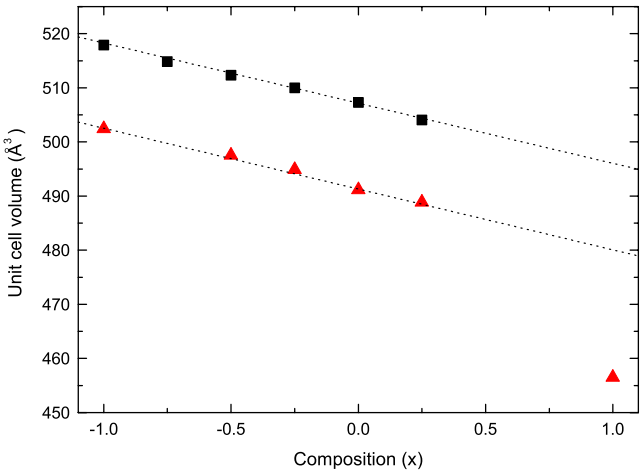

Figure 2. Calculated unit cell volume V (solid square) as a function of the composition x compared with the experimental ones (solid triangle). The experimental data are taken from [21].

of Mo–O–Mo, Fe–O–Fe, and Fe–O–Mo are all 180° from $x = -1$ to 0.25. We also plot the variation of the unit cell volume V as a function of composition x in figure 2 (remembering that GGA [20] is likely to overestimate the volume by 2–3%). It is interesting to note that the variation of V over the range of compositions ($-1 \leqslant x \leqslant 0.25$) studied here is linear with the composition x. However, the extrapolation of this linear trend to the $x = 1$ end point is in complete disagreement with the observed result for $SrFeO_3$, suggesting a drastic or sudden change of valency between $x = 0.25$ and 1 consistent with the fact that Fe is in the Fe $^{4+}$ state in $SrFeO_3$ (i.e. $x = 1$) and in the Fe^{3+} state in Sr_2FeMoO_6 (i.e. $x = 0$). A substitution of Mo^{5+} by Fe^{3+} or *vice versa*, as in $Sr_2Fe_{1+x}Mo_{1-x}O_6$ with $x \neq 0$, cannot satisfy the charge neutrality without changing the valency of Mo, provided Fe remains in the trivalent state. Mo is known to readily adopt a valence state between 4+ and 6+. Simple considerations then show that Fe can remain in the trivalent state for $-1 \leqslant x \leqslant \frac{1}{3}$ with Mo continuously changing its valency from Mo^{6+} for $x = 1/3$ to Mo^{4+} for $x = -1$. This suggests that Fe cannot retain its trivalent state for $x \geqslant 1/3$, as Mo cannot take up a valency larger than 6+. Thus, it appears that a systematic and continuous change in the lattice parameters for $-1 \leqslant x \leqslant 0.25$ is due to the progressive replacement of Fe by Mo, retaining Fe in the trivalent state, while the discontinuous change in the lattice parameter for $SrFeO_3$ is due to the change of Fe valency [21].

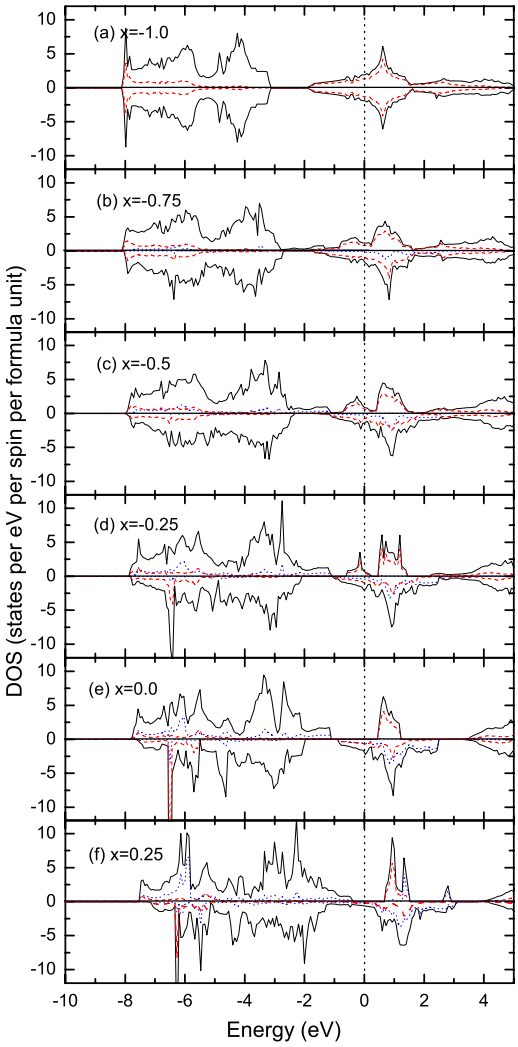

Figure 3. Total (solid line) densities of states and partial densities of states of Mo4 d (dashed line) and Fe3 d (dotted line) in $Sr_2Fe_{1+x}Mo_{1-x}O_6$ using GGA + U method. The energy zero is taken at the Fermi level. The upper halves of each panel display the spin-up states and the lower halves the spin-down states.

3.2. Electronic structure

The spin-polarized GGA + U calculations give a metallic ground state from $x = -1.0$ to -0.25 and a half-metallic ground state from $x = 0.0$ to 0.25 in $Sr_2Fe_{1+x}Mo_{1-x}O_6$, which are in agreement with experiments [21]. In figure 3, we show the calculated total density of states (DOS) and partial Fe 3d

and Mo 4d DOS for different compositions. For our discussion of the DOS, which is limited to an energy window of −8 eV to about 2 eV, we shall be primarily concerned with the Fe d, Mo d, and O p states, since the Sr-derived states appear higher in energy. $SrMoO_3$, i.e. the composition $x = -1$ (see figure 3(a)), is known to be a Pauli paramagnetic band metal [22], which is consistent with our DOS calculation. For the composition $x = 0$ (see figure 3(e)), the down-spin conduction band crossing the Fermi level (E_F) is dominated by the admixture of Fe t_{2g}, Mo t_{2g}, and oxygen p states; the up-spin band below E_F is mostly due to the Fe 3d and the O 2p states and the up-spin band just above the Fermi level is mostly of Mo t_{2g} state origin. The generic features of the DOS for $x = 0$ are consistent with previous results [2, 23, 24]. In the Fe-deficient regime ($x < 0$) (see figures 3(b)–(d)) where Mo replace some Fe sites, some Mo 4d states fill up the gap present between the Fe e_g and Mo t_{2g} spin-up states in the ordered sample which destroy the half-metallic ground state; with the Fe ion being in the high-spin d^5 state, the spin-up Fe states are completely filled, lying below the Fermi energy. In the Fe-rich regime ($x > 0$) where Fe replace some Mo sites (see figure 3(f)), the Fe d states appear in the spin-down channel below the Fermi energy and a weakening of the hybridization of Fe t_{2g}, Mo t_{2g}, and oxygen p states crossing the Fermi level; moreover, two peaks of Fe d states appear in the spin-up channel above the Fermi level. Obviously, a very sharp peak appears in the spin-down channel below E_F (about −6.4 eV) from $x = -0.25$ to 0.25, which is associated with the enhanced coupling of the O 2p and the transition-metal 3d state. We can note that there is no polarization of the states at and near E_F for $x = -1$ ($SrMoO_3$) and partial polarization for $x = -0.75$, −0.5, and $x = -0.25$, in contrast to the 100% polarization in the ordered ($x = 0$) sample. Furthermore, for $x = 0.25$ the DOS is very low, crossing the Fermi level, and the resistivity in some experiments [25] shows semiconducting behavior for $x \geqslant 0.2$.

In order to understand the effects of the surrounding atoms (see table 2), we also plot the site-projected DOS of Mo3′ d and Mo2 d for $x = -0.25$ and Fe4 d and Fe1′ d for $x = 0.25$ in figure 4. For the Mo3′ atom, the chemical environments are completely different from Mo2, we note a strong splitting of the t_{2g} states caused by the hybridization and the up-spin Mo t_{2g} states become partially occupied. For Mo2 atom, the chemical environments are the same as the Mo in the fully ordered compound, a sharp narrow band having contributions from Mo e_g states (at about −6.5 eV) appears in the spin-down channel far below the Fermi level and the down-spin t_{2g}, due to the hybridization with oxygen p and Fe t_{2g} in particular, acquires a large bandwidth (from about −7 to 1 eV). For Fe1′ atoms, the spin-down states (from −6.2 to −5.2 eV) are situated below the Fermi level, while the spin-up bands show a maximum above the Fermi level. It is also clear that the exchange splitting of Fe4 d states is weaker than that of Fe1′ atom because of different surroundings.

3.3. Magnetic properties

The calculated total magnetic moments (μ_T) for $Sr_2Fe_{1+x}Mo_{1-x}O_6$ are listed in table 1. The magnetic structures for $x \leqslant 0$ are found to be the ferromagnetic (FM) state while the magnetic structure for $x = 0.25$ is the ferrimagnetic (FIM) state (which is 0.68 eV lower in energy than the FM state) where the Fe spins are aligned ferromagnetically if the Fe are in the correct positions, and antiferromagnetically if the Fe ions occupy Mo sites. The μ_T shows the remarkable behavior of first increasing nearly linearly with x up to $x = 0$ and then decreasing once again with x, which is consistent with experiment [21]. However, the magnitude of the μ_T is different from the experimental value [21], which may be due to the antisite disorder in the real system [26]. For the $x \leqslant 0$ regime, μ_T increases with x primarily because the number of local moments increases and all Fe moments are ferromagnetically

Table 2. The atoms in parenthesis show the atoms which were replaced, and the atoms with ′ mean that they are not in the correct sites. The third and fourth columns give the nearest and the next-nearest number of Fe and/or Mo neighbors. The last column gives the magnetic moment at various inequivalent sites.

x	Sites	*nn*	*nnn*	Magnetic moment (μ_B)
−1.0	Mo/Mo′	6Mo	6Mo′	0.00
−0.75	Fe1(Mo1′)	6Mo	6Mo′	3.914
	Mo2′	6Mo	4Fe + 8Mo′	0.286
	Mo3′	6Mo	4Fe + 8Mo′	0.289
	Mo4′	6Mo	4Fe + 8Mo′	0.289
	Mo1	2Fe + 4Mo′	12Mo	−0.064
	Mo2	2Fe + 4Mo′	12Mo	−0.066
	Mo3	6Mo′	12Mo	−0.026
	Mo4	2Fe + 4Mo′	12Mo	−0.067
−0.5	Fe1(Mo1′)	6Mo	4Fe + 8Mo′	3.917
	Mo2′	6Mo	8Fe + 4Mo	0.498
	Mo3′	6Mo	8Fe + 4Mo	0.498
	Fe4(Mo4′)	6Mo	4Fe + 8Mo′	3.918
	Mo1	2Fe + 4Mo′	12Mo	0.059
	Mo2	4Fe + 2Mo′	12Mo	−0.326
	Mo3	2Fe + 4Mo′	12Mo	0.059
	Mo4	4Fe + 2Mo′	12Mo	−0.326
−0.25	Fe1(Mo1′)	6Mo	8Fe + 4Mo′	3.926
	Fe2(Mo2′)	6Mo	8Fe + 4Mo′	3.925
	Mo3′	6Mo	12Fe	0.583
	Fe4(Mo4′)	6Mo	8Fe + 4Mo′	3.924
	Mo1	4Fe + 2Mo′	12Mo	−0.129
	Mo2	6Fe	12Mo	−0.573
	Mo3	4Fe + 2Mo′	12Mo	−0.130
	Mo4	4Fe + 2Mo′	12Mo	−0.129
0	Fe1(Mo1′)	6Mo	12Fe	3.934
	Fe2(Mo2′)	6Mo	12Fe	3.934
	Fe3(Mo3′)	6Mo	12Fe	3.932
	Fe4(Mo4′)	6Mo	12Fe	3.935
	Mo1	6Fe	12Mo	−0.398
	Mo2	6Fe	12Mo	−0.396
	Mo3	6Fe	12Mo	−0.397
	Mo4	6Fe	12Mo	−0.398
0.25	Fe1(Mo1′)	2Fe′ + 4Mo	12Fe	4.006
	Fe2(Mo2′)	2Fe′ + 4Mo	12Fe	4.006
	Fe3(Mo3′)	2Fe′ + 4Mo	12Fe	4.006
	Fe4(Mo4′)	6Mo	12Fe	4.023
	Fe1′ (Mo1)	6Fe	12Mo	−3.931
	Mo2	6Fe	4Fe′ + 8Mo	−0.068
	Mo3	6Fe	4Fe′ + 8Mo	−0.068
	Mo4	6Fe	4Fe′ + 8Mo	−0.068

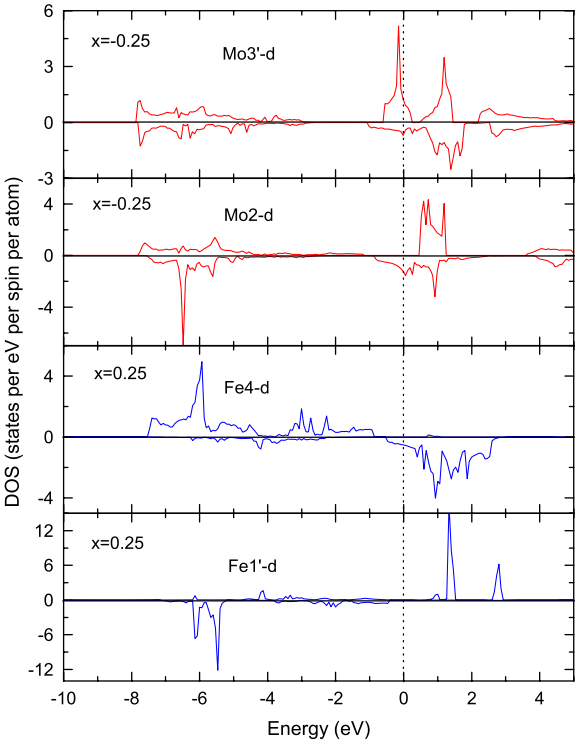

Figure 4. Site-projected density of states of the d component of Mo3′ and Mo2 for $x = -0.25$ and Fe4 and Fe1′ for $x = 0.25$ in $Sr_2Fe_{1+x}Mo_{1-x}O_6$. The energy zero is taken at the Fermi level. The upper halves of each panel display the spin-up states and the lower halves the spin-down states.

coupled. In the regime $x \geqslant 0$, as the Fe content increases, we find a rapid decrease of μ_T. This is readily understood in terms of the additional Fe being necessarily connected to the next Fe by 180° Fe–O–Fe bonds and, consequently, being antiferromagnetically coupled.

Table 2 shows the magnetic moments of inequivalent Fe and Mo (labeled in figure 1), and the number of Fe and Mo atoms in various neighbor shells differ from that of the ordered arrangement. We notice that the magnetic moments of Fe increase from 3.914 μ_B to 3.934 μ_B in the Fe-deficient regime ($x < 0$) and increase from 3.934 μ_B at $x = 0$ to 4.006 μ_B at $x = 0.25$. The increase of the magnetic moment of Fe in the Fe-deficient regime can be explained by the decreasing of the Fe–O–Mo bond length (see table 1). The increase of the magnetic moment of Fe from $x = 0.0$ to 0.25 may be explained by the strong antiferromagnetic (AFM) super-exchange interaction between the Fe at the correct sites and the Fe at the Mo sites, which enhances the ferromagnetism in the original Fe sublattice. The magnetic moments of Mo at the Fe sites, for the $x < 0$ regime, increase from about 0.289 μ_B to 0.583 μ_B, which is strongly influenced by the number of the Fe atoms in the next nearest-neighbor shell. The absolute magnetic moments of Mo at the correct sites, for the $x \leqslant 0$ regime, are strongly influenced by the number of Fe atoms in the nearest-neighbor shell; the higher the number of Fe atoms in the nearest-neighbor shell surrounding each Mo atom, the larger the absolute magnetic moment. The absolute magnetic moments of Mo at the correct sites, for the $x \geqslant 0$ regime, are influenced by the number of Mo/Fe atoms in the next nearest-neighbor shell. Additionally, the magnetic moments of Mo and Fe are also influenced by the Fe content, which can also see in the spin density maps (figures 5(a) and (b)). To understand the local magnetic moment of Mo, we note that the local magnetic moment of an element is determined by two factors: the occupation of the corresponding spin-up and spin-down bands and the hybridization of the states with other occupied and unoccupied states. The magnetic moment at the Mo site is merely induced by the Fe magnetic moment through the hybridization between the Fe 3d, Mo 4d and O 2p states. For example, for the local magnetic moment of Mo3′ and Mo2 at $x = -0.25$, the majority- and minority-spin channels of Mo3′ and Mo2 are not equally filled (see figure 4), resulting in positive and negative magnetic moments, respectively. A general feature for the entire $Sr_2Fe_{1+x}Mo_{1-x}O_6$ family is that the oxygen atoms also possess small magnetic moments which originate from Fe d, Mo d and O p hybridization. The magnetic moments at O atoms range from 0 to 0.12 μ_B and the moments at O are directed parallel to the majority-spin channel of Fe atoms. These can also be observed in figure 5. In figures 5(a) and (b), the Fe atoms are ferromagnetically coupled, inducing the spin polarization of Mo and oxygen sites significantly. The spin density distribution also demonstrates that the spin moments of Fe and Mo are mainly localized at nuclear sites and are coupled antiferromagnetically. The roughly spherical distributed positive spin densities at Fe sites indicate the nearly half-filled 3d orbitals, while the occupied Mo 4d orbital is mainly composed of down-spin t_{2g} electrons. Figure 5(c) shows the AFM interaction between Fe1 and Fe1′ and the negligibly small spin polarization of Mo and oxygen atoms. The spin density distribution at $x = 0$ is in agreement with published works [27].

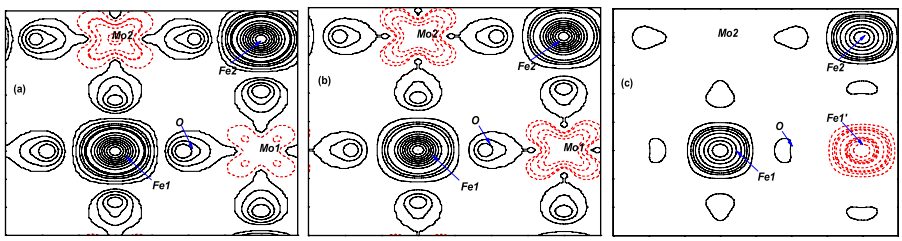

Figure 5. Contour plot of the spin density in the [100] plane for $Sr_2Fe_{1+x}Mo_{1-x}O_6$ at (a) $x = -0.25$, (b) $x = 0$, and (c) $x = 0.25$. Solid black lines represent positive charge densities and dashed red lines indicate negative charge density.

4. Conclusions

In conclusion, we have performed a study of the structural, electronic, and magnetic properties of $Sr_2Fe_{1+x}Mo_{1-x}O_6$ ($-1 \leqslant x \leqslant 0.25$) using first-principles density functional theory within the generalized gradient approximation (GGA) + U schemes. The crystal structure of the compounds has a cubic lattice for $x = -1$ and 0.25 while the structure of the compounds has a tetragonal lattice from $x = -0.75$ to 0.0. It is interesting to note that the variation of V over the range of compositions ($-1 \leqslant x \leqslant 0.25$) studied here is linear with the composition x. Our spin-polarized calculations give a metallic ground state for $x < 0$ regime and a half-metallic ground state for $x \geqslant 0$ regime. The magnetic structures for $x \leqslant 0$ are found to be the ferromagnetic state. The magnetic structure for $x = 0.25$ is the ferrimagnetic state where any Fe at the Mo crystallographic site is coupled antiparallel to the Fe moments at the correct site. The magnetic moment direction and magnitude of Mo are found to be related to the number of Fe and Mo sites in the nearest- and next-nearest neighbor shell. Additionally, the magnetic moments of Fe and Mo are also influenced by the Fe content. Contrary to the result of a recent quantum-mechanical band-structure study [8], the reduction in the total magnetic moment is mainly caused by antiferromagnetically coupled Fe pairs whenever Fe–O–Fe bonds are generated, which is in agreement with classical Monte Carlo simulations [7]. Our results resolve the conflicting views proposed earlier concerning the magnetic structure of such double perovskite oxides.

Acknowledgment

Numerical calculation was carried out using the facilities of the Department of Physics in Nanjing Normal University.

References

[1] See, for example Tokura Y (ed) 2000 *Colossal Magnetoresistive Oxides* (Amsterdam: Gordon and Breach)
[2] Kobayashi K-I, Kimura T, Sawada H, Terakura K and Tokura Y 1998 *Nature* **395** 677
[3] Sarma D D, Mahadevan P, Saha-Dasgupta T, Ray S and Kumar A 2000 *Phys. Rev. Lett.* **85** 2549
[4] Ray S, Kumar A, Sarma D D, Cimino R, Turchini S, Zennaro S and Zema N 2001 *Phys. Rev. Lett.* **87** 097204
[5] Tomioka Y, Okuda T, Okimoto Y, Kumai R, Kobayashi K I and Tokura Y 2000 *Phys. Rev.* B **61** 422
[6] Ray S, Kumar A, Majumdar S, Sampathkumaran E V and Sarma D D 2001 *J. Phys.: Condens. Matter* **13** 607
[7] Ogale A S, Ramesh R and Venkatesan T 1999 *Appl. Phys. Lett.* **75** 537
[8] Saha-Dasgupta T and Sarma D D 2001 *Phys. Rev.* B **64** 064408
[9] García-Hernández M, Martínez J L, Martínez-Lope M J, Casais M T and Alonso J A 2001 *Phys. Rev. Lett.* **86** 2443
[10] Blöchl P E 1994 *Phys. Rev.* B **50** 17953
[11] Kresse G and Joubert D 1999 *Phys. Rev.* B **59** 1758
[12] Kresse G and Furthmuller J 1996 *Phys. Rev.* B **54** 11169
[13] Kresse G and Furthmuller J 1996 *Comput. Mater. Sci.* **6** 15
[14] Anisimov V I, Zaanen J and Andersen O K 1991 *Phys. Rev.* B **44** 943
[15] Rohrbach A, Hafner J and Kresse G 2003 *J. Phys.: Condens. Matter* **15** 979
[16] Liechtenstein A I, Anisimov V I and Zaanen J 1995 *Phys. Rev.* B **52** R5467
[17] Dudarev S L, Botton G A, Savrasov S Y, Humphreys C J and Stutton A P 1998 *Phys. Rev.* B **57** 1505
[18] Monkhorst H J and Pack J D 1976 *Phys. Rev.* B **13** 5188
[19] Howard C, Kennedy B J and Woodward P M 2003 *Acta Crystallogr.* B **59** 463
[20] Häussermann U, Blomqvist H and Noréus D 2002 *Inorg. Chem.* **41** 3684
[21] Topwal D, Sarma D D, Kato H, Tokura Y and Avignon M 2006 *Phys. Rev.* B **73** 094419
[22] Agarwal R, Singh Z and Venugopal V 1999 *J. Alloys Compounds* **282** 231
[23] Moritomo Y, Xu Sh, Akimoto T, Machida A, Hamada N, Ohoyama K, Nishibori E, Takata M and Sakata M 2000 *Phys. Rev.* B **62** 14224
[24] Saha-Dasgupta T and Sarma D D 2001 *Phys. Rev.* B **64** 064408
[25] Liu G Y, Rao G H, Feng X M, Yang H F, Ouyang Z W, Liu W F and Liang J K 2003 *Physica* B **334** 229
Liu G Y, Rao G H, Feng X M, Yang H F, Ouyang Z W, Liu W F and Liang J K 2003 *J. Alloys Compounds* **353** 42
Liu G Y, Rao G H, Feng X M, Yang H F, Ouyang Z W, Liu W F and Liang J K 2003 *J. Phys.: Condens. Matter* **15** 2053
[26] Allub R, Navarro O, Avignon M and Alascio B 2002 *Physica* B **320** 13
Carvajal E, Navarro O, Allub R, Avignon M and Alascio B 2004 *J. Magn. Magn. Mater.* **273** 1774
Carvajal E, Navarro O, Allub R, Avignon M and Alascio B 2005 *Eur. Phys. J.* B **48** 179
[27] Jeng H-T and Guo G Y 2003 *Phys. Rev.* B **67** 094438